

# Negative refraction, negative phase velocity, and counterposition

Tom G. Mackay<sup>1</sup>

*School of Mathematics and Maxwell Institute for Mathematical Sciences  
University of Edinburgh, Edinburgh EH9 3JZ, UK*

and

*NanoMM — Nanoengineered Metamaterials Group  
Department of Engineering Science and Mechanics  
Pennsylvania State University, University Park, PA 16802–6812, USA*

Akhlesh Lakhtakia<sup>2</sup>

*NanoMM — Nanoengineered Metamaterials Group  
Department of Engineering Science and Mechanics  
Pennsylvania State University, University Park, PA 16802–6812, USA*

## Abstract

The planewave response of a linear passive material generally cannot be characterized by a single scalar refractive index, as directionality of energy flow and multiple wavevectors may need to be considered. This is especially significant for materials which support negative refraction, negative phase velocity, and counterposition. By means of a numerical example based on a commonly studied bianisotropic material, our theoretical investigation revealed that: (i) negative (positive) refraction can arise even though the phase velocity is positive (negative); (ii) counterposition can arise in instances of positive and negative refraction; (iii) the phase velocity and time-averaged Poynting vectors can be mutually orthogonal; and (iv) whether or not negative refraction occurs can depend upon the state of polarization and angle of incidence. A further numerical example revealed that negative phase velocity and positive refraction can co-exist even in a simple isotropic dielectric material.

## 1 Introduction

Negatively refracting materials have been subjected to intense interest since the first experimental demonstration of a negatively refracting isotropic dielectric-magnetic material at the turn of this century [1, 2]. The enhanced scope for negative refraction in anisotropic materials [3, 4], and in materials which exhibit either isotropic [5, 6, 7] or anisotropic [8] magnetoelectric coupling, has been widely reported upon. Indeed, bianisotropy may be responsible for unexplained features in certain materials which were taken to be isotropic dielectric-magnetic materials [9].

We confine ourselves here to linear passive materials. The characterization of negative refraction in anisotropic and bianisotropic materials should be expected to be much more complicated than in isotropic dielectric-magnetic materials, as the effects of directionality, magnetoelectric coupling, and two refraction wavevectors need to be considered [10]. However, it is often overlooked that even in an isotropic dielectric material the effects of directionality can be important if *nonuniform* plane waves are considered. Negative phase velocity (NPV) — which means that the phase velocity of a plane wave casts a negative projection onto the time-averaged Poynting vector — is commonly taken as convenient indication of the propensity for negative refraction [11, 12]. For uniform plane waves in isotropic dielectric-magnetic materials, the phase velocity and time-averaged Poynting vector are either parallel or antiparallel. Accordingly, as regards uniform planewave propagation, *negative refraction* and *NPV* are held to be effectively synonymous terms

---

<sup>1</sup>E-mail: T.Mackay@ed.ac.uk.

<sup>2</sup>E-mail: akhlesh@psu.edu

for these materials. But for nonuniform plane waves, the time-averaged Poynting vector and the phase velocity vector are not necessarily parallel or antiparallel, even in isotropic dielectric materials [13]. The introduction of anisotropy or bianisotropy further complicates the issue, with the phase velocity and time-averaged Poynting vector being generally neither parallel nor antiparallel, for both uniform and nonuniform plane waves. Thus, NPV should not be generally assumed to be a definite signature of the capability to exhibit negative refraction.

For many practical applications, the direction of energy flow, as delineated by the time-averaged Poynting vector, and its deflection at the planar boundary between two different mediums may be more significant than the deflection of the wavevector. It is quite possible for the real part of a refraction wavevector and its associated time-averaged Poynting vector to be oriented on opposite sides of the normal to a planar interface. This counterposition of the real part of the refraction wavevector and the time-averaged Poynting vector has been theoretically demonstrated as taking place in certain anisotropic [14, 15, 16] and bianisotropic [17] materials. Furthermore, counterposition can also arise for nonuniform planewave propagation in certain isotropic dielectric materials, as we describe later in this paper.

Very recently there have been several reports of bianisotropic materials which may possess structural chirality and exhibit a “negative index” [18, 19, 20, 21], including a commentary on this topic [22]. The “negative index” relates to the real part of a wavenumber (relative to that in vacuum), typically corresponding to propagation in one direction only, for one polarization state only. However, the planewave responses of bianisotropic materials is not at all adequately represented that simply: different directions of propagation, different polarization states, and the relationship to the time-averaged Poynting vector need to be considered too. In contrast, we note that there are some studies in which bianisotropic aspects are taken into account better [23, 24, 25]. In the remainder of this paper, we highlight the complications that can arise in the planewave response of such a bianisotropic material; furthermore, we demonstrate that some of these complications can actually be exhibited by relatively simple materials, such as an isotropic dielectric material. In so doing, we report on important distinctions between negative refraction, NPV, and counterposition which have not been appreciated hitherto.

## 2 Plane waves in a bianisotropic material

Let us consider the Lorentz-reciprocal [26] bianisotropic material described by the constitutive relations

$$\left. \begin{aligned} \underline{D} &= \underline{\epsilon} \cdot \underline{E} + \underline{\xi} \cdot \underline{H} \\ \underline{B} &= \underline{\zeta} \cdot \underline{E} + \underline{\mu} \cdot \underline{H} \end{aligned} \right\}, \quad (1)$$

wherein

$$\begin{aligned} \underline{\epsilon} &= \epsilon_0 \begin{pmatrix} \epsilon_x & 0 & 0 \\ 0 & \epsilon_y & 0 \\ 0 & 0 & \epsilon_z \end{pmatrix}, & \underline{\xi} &= \frac{1}{c_0} \begin{pmatrix} 0 & 0 & 0 \\ 0 & 0 & 0 \\ 0 & -i\xi & 0 \end{pmatrix}, \\ \underline{\zeta} &= \frac{1}{c_0} \begin{pmatrix} 0 & 0 & 0 \\ 0 & 0 & i\xi \\ 0 & 0 & 0 \end{pmatrix}, & \underline{\mu} &= \mu_0 \begin{pmatrix} \mu_x & 0 & 0 \\ 0 & \mu_y & 0 \\ 0 & 0 & \mu_z \end{pmatrix}, \end{aligned} \quad (2)$$

with  $\epsilon_0$  and  $\mu_0$  being the permittivity and permeability of vacuum, respectively, and  $c_0 = 1/\sqrt{\epsilon_0\mu_0}$ . These particular constitutive relations were chosen because they have been used to describe a material assembled from layers of split-ring resonators [27]. This general configuration is a popular one within the negative refraction community [21, 20, 25], but its origins predate the current surge of interest in negative refraction [28]. The term *pseudochiral omega material* may be used to describe this material [29].

Suppose that a material described by (1) and (2) occupies the half-space  $z > 0$ , while the half-space  $z < 0$  is a vacuum. We confine ourselves to propagation in the  $xz$  plane. In the half-space  $z < 0$ , a plane

wave with field phasors

$$\left. \begin{aligned} \underline{E}(\underline{r}) &= \underline{E}_0 \exp [ik_0 (x \sin \psi + z \cos \psi)] \\ \underline{H}(\underline{r}) &= \underline{H}_0 \exp [ik_0 (x \sin \psi + z \cos \psi)] \end{aligned} \right\} \quad (3)$$

is incident on the interface  $z = 0$ , where the free-space wavenumber  $k_0 = \omega \sqrt{\epsilon_0 \mu_0}$ , with  $\omega$  being the angular frequency. As the incident plane wave transports energy towards the interface, the angle  $\psi \in [0, \pi/2)$  so that the real-valued scalar

$$\kappa = k_0 \sin \psi \in [0, k_0) . \quad (4)$$

Two refracted plane waves must exist in the half-space  $z > 0$ . Let us represent these plane waves by the phasors

$$\left. \begin{aligned} \underline{E}(\underline{r}) &= \underline{E}_j \exp (i \underline{k}_j \cdot \underline{r}) \\ \underline{H}(\underline{r}) &= \underline{H}_j \exp (i \underline{k}_j \cdot \underline{r}) \end{aligned} \right\}, \quad (j = 1, 2), \quad (5)$$

wherein the wavevectors

$$\underline{k}_j = \kappa \hat{x} + k_{zj} \hat{z}, \quad (6)$$

with  $k_{zj} \in \mathbb{C}$  in general. Thus, the plane waves in the half-space  $z > 0$  are generally nonuniform. The scalars  $k_{zj}$  are found by combining the constitutive relations (1) and (2) and the planewave phasors (5) with the Maxwell curl postulates. Thereby, we find [10]

$$\underline{\underline{L}} \cdot \underline{E}_j = \underline{0}, \quad (j = 1, 2), \quad (7)$$

with the dyadic

$$\underline{\underline{L}} = \left( \underline{k}_j \times \underline{\underline{I}} + \omega \underline{\underline{\xi}} \right) \cdot \underline{\underline{\mu}}^{-1} \cdot \left( \underline{k}_j \times \underline{\underline{I}} - \omega \underline{\underline{\zeta}} \right) + \omega^2 \underline{\underline{\epsilon}}. \quad (8)$$

The dispersion relation  $\det \underline{\underline{L}} = 0$  yields the two wavenumbers

$$\left. \begin{aligned} k_{z1} &= k_0 \sqrt{\mu_x \left( \epsilon_y - \frac{\kappa^2}{\mu_z k_0^2} \right)} \\ k_{z2} &= k_0 \sqrt{\frac{\epsilon_x}{\epsilon_z} \left[ (\epsilon_z \mu_y - \xi^2) - \frac{\kappa^2}{k_0^2} \right]} \end{aligned} \right\}. \quad (9)$$

In these two relations, the square roots must be evaluated such that both refracted plane waves transport energy away from the interface  $z = 0$  in the half-space  $z > 0$ .

In order to establish the energy flow associated with the refraction wavevectors  $\underline{k}_j$ , the time-averaged Poynting vectors

$$\begin{aligned} \underline{P}_j &= \frac{1}{2} \exp [-2 \operatorname{Im} (\underline{k}_j) \cdot \underline{r}] \operatorname{Re} \left\{ \underline{E}_j \times \left[ \frac{1}{\omega} \left( \underline{\underline{\mu}}^{-1} \right)^* \right. \right. \\ &\quad \left. \left. \cdot \left( \underline{k}_j^* \times \underline{E}_j^* - \omega \underline{\underline{\zeta}}^* \cdot \underline{E}_j^* \right) \right] \right\}, \quad (j = 1, 2), \end{aligned} \quad (10)$$

have to be considered. Both  $\underline{P}_1$  and  $\underline{P}_2$  lie in the  $xz$  plane; furthermore,  $\underline{E}_1$  is directed along the  $y$  axis whereas  $\underline{E}_2$  lies in the  $xz$  plane.

Let us now consider a specific numerical example in which the constitutive parameters for the bianisotropic material occupying the half-space  $z > 0$  are:  $\epsilon_x = 0.1 + 0.03i$ ,  $\epsilon_y = 0.14 + 0.02i$ ,  $\epsilon_z = 0.13 + 0.07i$ ;  $\mu_x = -0.29 + 0.09i$ ,  $\mu_y = -0.18 + 0.03i$ ,  $\mu_z = -0.17 + 0.6i$ ; and  $\xi = 0.11 + 0.05i$ . These particular values of the constitutive parameters are chosen in order to highlight the complexity of planewave response that can be exhibited by bianisotropic materials. Since these materials are artificially constructed materials, the range of values that their constitutive parameters can adopt is vast. There is no theoretical barrier to

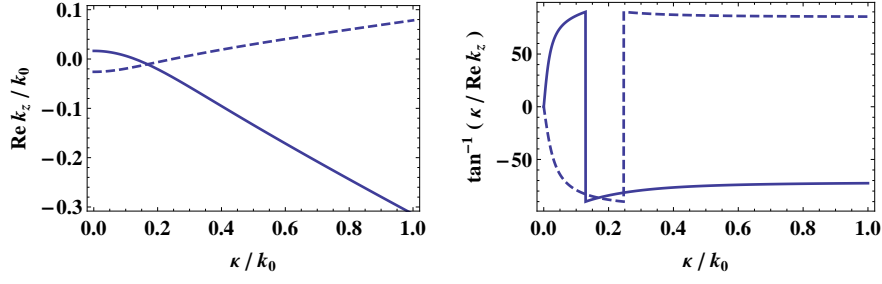


Figure 1: (top) Real part of  $k_{zj}/k_0$  and (bottom) the angle (in degree) between the real part of  $\underline{k}_j$  and the positive  $z$  axis, both plotted against  $\kappa/k_0$ . The solid curves correspond to  $j = 1$ , and the dashed curves to  $j = 2$ . As  $\text{Im } k_{zj} > 0$  for all  $\kappa/k_0 \in [0, 1)$  and both values of  $j$ , the imaginary parts of  $k_{z1}/k_0$  and  $k_{z2}/k_0$  have not been plotted here.

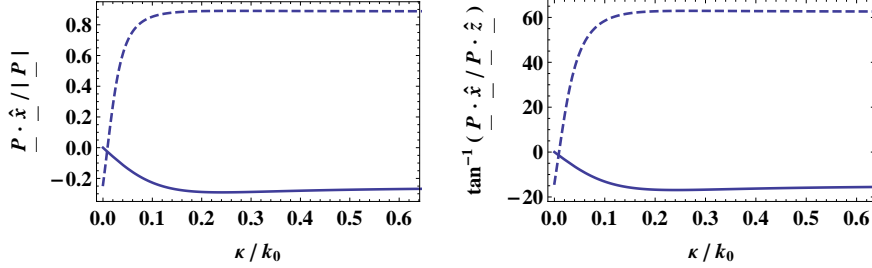


Figure 2: (top) The  $x$  component of the normalized time-averaged Poynting vector and (bottom) the angle (in degree) between the time-averaged Poynting vector and the positive  $z$  axis, both plotted against  $\kappa/k_0$ . The solid curves correspond to  $j = 1$ , and the dashed curves to  $j = 2$ . As  $\hat{\underline{z}} \cdot \underline{P}_j > 0$  for all  $\kappa/k_0 \in [0, 1)$  and both values of  $j$ , those quantities have not been plotted here.

the particular values chosen here: these describe a dissipative pseudo-chiral omega material. It is through accessing unconventional values of the constitutive parameters that we determine if metamaterials may exhibit their exotic, and potentially useful, properties.

In Fig. 1, the real part of  $k_{zj}/k_0$ , ( $j = 1, 2$ ), is plotted as a function of  $(\kappa/k_0) \in [0, 1)$ . As the imaginary parts of both  $k_{z1}$  and  $k_{z2}$  turned out to be positive, both refracted plane waves must attenuate as  $z \rightarrow \infty$ , in consonance with our understanding of a passive medium. Also plotted in Fig. 1 is the angle between the real part of  $\underline{k}_j$ , ( $j = 1, 2$ ), and the positive  $z$  axis. The refracted plane wave labeled 1 is positively refracted for  $0 < (\kappa/k_0) < 0.14$  but negatively refracted for  $0.14 < (\kappa/k_0) < 1$ . Additionally, the refracted plane wave labeled 2 is negatively refracted for  $0 < (\kappa/k_0) < 0.22$  but positively refracted for  $0.22 < (\kappa/k_0) < 1$ .

The normalized  $x$  component of the time-averaged Poynting vectors for both refracted plane waves are plotted against  $(\kappa/k_0)$  in Fig. 2. The angle between  $\underline{P}_j$ , ( $j = 1, 2$ ), and the positive  $z$  axis is also plotted. The  $z$  components of  $\underline{P}_1$  and  $\underline{P}_2$  are positive for all  $(\kappa/k_0) \in [0, 1)$ , in accordance with the rule to evaluate the square roots in (9). But, whereas the  $x$  component of  $\underline{P}_1$  is negative for all  $(\kappa/k_0) \in [0, 1)$ , the  $x$  component of  $\underline{P}_2$  is negative only for  $(\kappa/k_0) \in [0, 0.01)$ . Therefore,  $\underline{P}_1$  always subtends a negative angle to the positive  $z$  axis whereas the sign of the angle that  $\underline{P}_2$  subtends depends on  $\kappa$ .

The phenomenon of counterposition [16] arises when the inequality

$$\text{Re}(k_{zj}) \hat{\underline{x}} \cdot \underline{P}_j < 0 \quad (11)$$

is satisfied. By comparing Figs. 1 and 2, we see that counterposition occurs for the refracted plane wave labeled 1 when  $0 < (\kappa/k_0) < 0.14$ . That is, the  $\kappa$ -range for counterposition coincides with the  $\kappa$ -range for

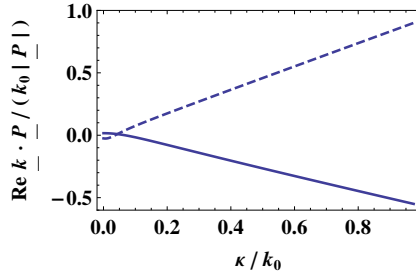


Figure 3: The quantity  $\text{Re}(\underline{k}_j) \cdot \underline{P}_j / (k_0 |\underline{P}_j|)$  plotted against  $(\kappa/k_0) \in [0, 1)$ . The solid curve corresponds to  $j = 1$ , and the dashed curve to  $j = 2$ .

positive refraction. However, this is not the case for the refracted plane wave labeled 2: here, counterposition occurs only for  $0.01 < (\kappa/k_0) < 0.22$ .

The quantity  $\text{Re}(\underline{k}_j) \cdot \underline{P}_j$  determines whether the phase velocity of the refracted plane wave labeled  $j$  is positive or negative. In Fig. 3, the quantities  $\text{Re}(\underline{k}_j) \cdot \underline{P}_j / (k_0 |\underline{P}_j|)$ , ( $j = 1, 2$ ), are plotted against  $(\kappa/k_0) \in [0, 1)$ . The phase velocity is negative for the refracted plane wave labeled 1 for  $0.07 < (\kappa/k_0) < 1$ , while for the refracted plane wave labeled 2 it is negative for  $0 < (\kappa/k_0) < 0.04$ . Thus, the  $\kappa$ -ranges for NPV do not coincide exactly with those for negative refraction. For example, consider  $\kappa = 0.1k_0$ : (i) The angle between  $\text{Re}\underline{k}_1$  and the  $+z$  axis is  $86^\circ$  while the angle between  $\underline{P}_1$  and the  $+z$  axis is  $-13^\circ$ . This refracted plane wave has NPV but it is positively refracted. (ii) The angle between  $\text{Re}\underline{k}_2$  and the  $+z$  axis is  $-79^\circ$  while the angle between  $\underline{P}_2$  and the  $+z$  axis is  $58^\circ$ . This plane wave has positive phase velocity but it is negatively refracted.

Our results are summarized in Tables 1 and 2 for the plane waves labeled 1 and 2, respectively. These tables include illustrations of the directions of  $\text{Re}\underline{k}_j$  and  $\underline{P}_j$ , ( $j = 1, 2$ ), for representative values of  $\kappa$ . In the Appendix we have confirmed that the corresponding reflection and transmission coefficients are nonzero.

### 3 A simple case: an isotropic dielectric material

An important point demonstrated in the preceding section is that, under certain circumstances, NPV and positive refraction can co-exist for the bianisotropic material under consideration. This co-existence of NPV and positive refraction has previously been predicted for certain photonic crystals [30] and nondissipative uniaxial dielectric mediums described by indefinite permittivity tensors [14] (as well as for certain active materials [31]). In fact, the independence of NPV and negative refraction is also manifest in simpler materials. Let us take, for example, the simple case where the half-space  $z > 0$  is occupied by an isotropic, dielectric material with relative permittivity scalar  $\epsilon$ . This represents the simplest specialization of (1) and (2). Here there is only one refraction wave vector, i.e.,  $\underline{k}_1 = \underline{k}_2$ , where  $|\underline{k}_{1,2}| = k_0\sqrt{\epsilon}$ , but the two associated time-averaged Poynting vectors, namely  $\underline{P}_1$  and  $\underline{P}_2$ , are generally distinct in terms of both magnitude and direction for  $\epsilon \in \mathbb{C}$ . As previously,  $\underline{P}_1$  corresponds to  $\underline{E}_1$  being perpendicular to the plane of incidence and  $\underline{P}_2$  corresponds to  $\underline{E}_2$  being parallel to the plane of incidence.

For the purposes of illustration, let us take the relative permittivity scalar  $\epsilon = -6 + 2.5i$ . A straightforward calculation reveals that the refraction is always positive for both perpendicular and parallel polarization states. Furthermore, when the electric field phasor is perpendicular to the plane of incidence, the phase velocity is positive and there is no counterposition, regardless of the value of  $\psi$ . Indeed, the time-averaged Poynting vector and the phase velocity are parallel for this polarization state. A different picture emerges when the electric field phasor is parallel to the plane of incidence: counterposition occurs for all  $\psi$  and the phase velocity changes from positive to negative as  $\psi$  increases in value, with the phase velocity being orthogonal to the time-averaged Poynting vector when  $\psi = 32^\circ$ .

The directions of the refracted wavevectors and the corresponding time-averaged Poynting vectors are

$(\kappa/k_0) \in$	Refraction	Counter-position	Phase velocity	$\underline{P}_1, \text{Re } \underline{k}_1$
$(0, 0.07)$	+ve	yes	+ve	
$\{0.07\}$	+ve	yes	ortho-gonal	
$(0.07, 0.14)$	+ve	yes	-ve	
$(0.14, 1)$	-ve	no	-ve	

Table 1: Ranges of values of  $\kappa$  for which the plane wave labeled 1 supports negative/positive refraction, counterposition and negative/positive/orthogonal phase velocity. The final column shows the directions in the  $z > 0$  half-space of  $\text{Re } \underline{k}_1$  (thick dashed arrows; blue in electronic version)  $\underline{P}_1$  (thick solid arrows; red in electronic version) for representative values of  $\kappa$ ; also shown are the directions of the wavevectors for the incident and reflected plane waves in the  $z < 0$  half-space (thin solid arrows; green in electronic version).

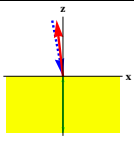
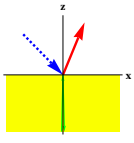
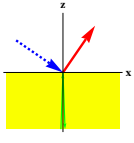
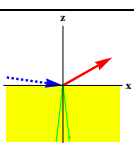
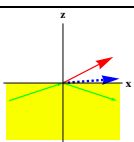
$(\kappa/k_0) \in$	Refraction	Counter-position	Phase velocity	$\underline{P}_2, \text{Re } \underline{k}_2$
$(0, 0.01)$	-ve	no	-ve	
$(0.01, 0.04)$	-ve	yes	-ve	
$\{0.04\}$	-ve	yes	ortho-gonal	
$(0.04, 0.22)$	-ve	yes	+ve	
$(0.22, 1)$	+ve	no	+ve	

Table 2: As Table 1 but for the plane wave labeled 2.

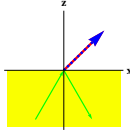
$(\kappa/k_0) \in$	Refraction	Counter-position	Phase velocity	$\underline{P}_1, \text{Re } \underline{k}_1$
$(0, 1)$	+ve	no	+ve	

Table 3: As Table 1 but the  $z > 0$  half-space is replaced by an isotropic dielectric material with a relative permittivity  $\epsilon = -6 + 2.5i$ . The plane wave is polarized perpendicular to the plane of incidence. Notice that here  $\text{Re } \underline{k}_1$  and  $\underline{P}_1$  are parallel.

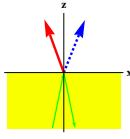
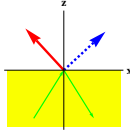
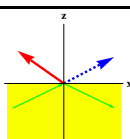
$(\kappa/k_0) \in$	Refraction	Counter-position	Phase velocity	$\underline{P}_2, \text{Re } \underline{k}_2$
$(0, 0.53)$	+ve	yes	+ve	
$\{0.53\}$	+ve	yes	ortho-gonal	
$(0.53, 1)$	+ve	yes	-ve	

Table 4: As Table 3 but the plane wave is polarized parallel to the plane of incidence.

illustrated in Tables 3 and 4 for both polarization states and for some representative values of  $\kappa$ .

## 4 Concluding remarks

The combination of anisotropy and magnetoelectric coupling can result in a much more complicated planewave response than is associated with isotropic dielectric-magnetic materials. This is especially significant when exotic constitutive parameters ranges — such as those associated with certain materials which support negative refraction — are considered. A further level of complication is introduced by considering nonuniform plane waves. The relationships among the three phenomenons of negative refraction, NPV, and counterposition highlight the complications. In particular, our investigation based on a pseudochiral omega material has revealed that: (a) negative refraction can arise even though the phase velocity is positive, and positive refraction can arise even though the phase velocity is negative; (b) counterposition can arise in instances of positive and negative refraction; (c) whether or not positive or negative refraction arises can depend upon the angle of incidence; and (d) at the transition from positive to negative phase velocity with increasing angle of incidence, the phase velocity and time-averaged Poynting vector are orthogonal to each other.

The exhibition of NPV in an isotropic dielectric material — which follows due to the consideration of nonuniform plane waves — is particularly noteworthy. If only uniform plane waves are considered then this outcome is impossible: magnetic properties or anisotropy, for example, would also be needed in order to support NPV [12, 14].

The findings reported herein further emphasize the importance of fully characterizing bianisotropic ma-



terials, instead of attempting to do so with a single scalar refractive index. Also, the complications that can be introduced by taking account of nonuniform plane waves, even in isotropic dielectric materials, are highlighted. The demonstration that NPV and negative refraction can arise independently of each other has highly significant consequences for researchers exploring the realm of materials which support negative refraction, bianisotropic or otherwise, and beyond.

## References

- [1] D. R. Smith, W. J. Padilla, D. C. Vier, S. C. Nemat-Nasser, and S. Schultz, *Phys. Rev. Lett.* **84**, 4184 (2000).
- [2] R. A. Shelby, D. R. Smith, and S. Schultz, *Science* **292**, 77 (2001).
- [3] L. Hu and Z. Lin, *Phys. Lett. A* **313**, 316 (2003).
- [4] M. K. Kärkkäinen, *Phys. Rev. E* **68**, 026602 (2003).
- [5] A. Lakhtakia, V. V. Varadan, and V. K. Varadan, *IEEE Trans. Electromag. Compat.* **28**, 90 (1986).
- [6] T. G. Mackay, *Microwave Opt. Technol. Lett.* **45**, 120 (2005); erratum **47**, 406 (2005).
- [7] C. Monzon and D. W. Forester, *Phys. Rev. Lett.* **95**, 123904 (2005).
- [8] T. G. Mackay and A. Lakhtakia, *Phys. Rev. E* **69**, 026602 (2004).
- [9] R. Marqués, F. Medina, and R. Rafii-El-Idrissi, *Phys. Rev. B* **65**, 144440 (2002).
- [10] T. G. Mackay and A. Lakhtakia, *Prog. Optics* **51**, 121 (2008).
- [11] M. W. McCall, A. Lakhtakia, and W. S. Weiglhofer, *Eur. J. Phys.* **23**, 353 (2002).
- [12] R. A. Depine and A. Lakhtakia, *Microwave Opt. Technol. Lett.* **41**, 315 (2004).
- [13] H. C. Chen, *Theory of Electromagnetic Waves*, (McGraw-Hill, New York, NY, USA, 1983).
- [14] P. A. Belov, *Microwave Opt. Technol. Lett.* **37**, 259 (2003).
- [15] Y. Zhang, B. Fluegel, and A. Mascarenhas, *Phys. Rev. Lett.* **91**, 157404 (2003).
- [16] A. Lakhtakia and M. W. McCall, *Optik* **115**, 28 (2004).
- [17] T. G. Mackay and A. Lakhtakia, *Microwave Opt. Technol. Lett.* **49**, 874 (2007).
- [18] E. Plum, J. Zhou, J. Dong, V. A. Fedotov, T. Koschny, C. M. Soukoulis, and N. I. Zheludev, *Phys. Rev. B* **79**, 035407 (2009).
- [19] S. Zhang, Y.-S. Park, J. Li, X. Lu, W. Zhang, and X. Zhang, *Phys. Rev. Lett.* **102**, 023901 (2009).
- [20] M. S. Rill, C. E. Kriegler, M. Thiel, G. von Freymann, S. Linden, and M. Wegener, *Opt. Lett.* **34**, 19 (2009).
- [21] M. S. Rill, C. Plet, M. Thiel, I. Staude, G. von Freymann, S. Linden, and M. Wegener, *Nature Mat.* **7**, 543 (2008).
- [22] M. Wegener and S. Linden, *Physics* **2**, 3 (2009).
- [23] V. V. Varadan and S. Puligalla, *URSI General Assembly* (New Delhi, 2005), paper BCDP.

- [24] S. A. Tretyakov, C. R. Simovski, and M. Hudlika, Phys. Rev. B **75**, 153104 (2007).
- [25] Z. Li, K. Aydin, and E. Ozbay, Phys. Rev. E **79**, 026610 (2009).
- [26] C. M. Krowne, IEEE Trans. Antennas Propagat. **32**, 1224 (1984).
- [27] X. Chen, B.-I. Wu, J. A. Kong, and T. M. Grzegorzczak, Phys. Rev. E **71**, 046610 (2005). Erratum **73** (2006), 019905(E).
- [28] M. M. I. Saadoun and N. Engheta, Microwave Opt. Technol. Lett. **5**, 184 (1992).
- [29] A. Serdyukov, I. Semchenko, S. Tretyakov, and A. Sihvola, *Electromagnetics of Bi-anisotropic Materials* (Gordon and Breach, Amsterdam, 2001), p.40.
- [30] P. A. Belov, C. R. Simovski, and S. A. Tretyakov, J. Commun. Technol. Electron. **49**, 1199 (2004).
- [31] A. Lakhtakia, T. G. Mackay, and J. B. Geddes III, Microwave Opt. Technol. Lett. **51**, 1230 (2009).

## Appendix

We present here the reflection and transmission coefficients corresponding to the reflection–transmission problem.

In terms of linearly polarized states, the incident plane wave is represented by the electric and magnetic phasors

$$\left. \begin{aligned} \underline{E}_i(\underline{r}) &= \left( a_s \underline{s} + a_p \underline{p}_+ \right) \exp [i (\kappa x + k_0 z \cos \psi)] \\ \underline{H}_i(\underline{r}) &= \frac{1}{\eta_0} \left( a_s \underline{p}_+ - a_p \underline{s} \right) \exp [i (\kappa x + k_0 z \cos \psi)] \end{aligned} \right\}, \quad z < 0, \quad (12)$$

where  $\eta_0 = \sqrt{\mu_0/\epsilon_0}$  and the unit vectors

$$\underline{s} = \hat{y}, \quad \underline{p}_\pm = \mp \hat{x} \cos \psi + \hat{z} \sin \psi. \quad (13)$$

The corresponding reflected plane wave is represented by

$$\left. \begin{aligned} \underline{E}_r(\underline{r}) &= \left( r_s \underline{s} + r_p \underline{p}_- \right) \exp [i (\kappa x - k_0 z \cos \psi)] \\ \underline{H}_r(\underline{r}) &= \frac{1}{\eta_0} \left( r_s \underline{p}_- - r_p \underline{s} \right) \exp [i (\kappa x - k_0 z \cos \psi)] \end{aligned} \right\}, \quad z < 0, \quad (14)$$

and the transmitted fields are written as

$$\left. \begin{aligned} \underline{E}_t(\underline{r}) &= t_1 \underline{s} \exp [i (\kappa x + k_{z1} z)] + t_2 \underline{p} \exp [i (\kappa x + k_{z2} z)] \\ \underline{H}_t(\underline{r}) &= t_1 \underline{\underline{\mu}}^{-1} \cdot \left( \frac{1}{\omega} \underline{k}_1 \times \underline{I} - \underline{\underline{\zeta}} \right) \cdot \underline{s} \exp [i (\kappa x + k_{z1} z)] \\ &\quad + t_2 \underline{\underline{\mu}}^{-1} \cdot \left( \frac{1}{\omega} \underline{k}_2 \times \underline{I} - \underline{\underline{\zeta}} \right) \cdot \underline{p} \exp [i (\kappa x + k_{z2} z)] \end{aligned} \right\}, \quad z > 0, \quad (15)$$

wherein vector

$$\underline{p} = \left( 1 + \left| \frac{[\underline{L}]_{1,1}}{[\underline{L}]_{1,3}} \right|^2 \right)^{-1/2} \left( \hat{x} - \frac{[\underline{L}]_{1,1}}{[\underline{L}]_{1,3}} \hat{z} \right) \quad (16)$$

satisfies  $\underline{p} \cdot \underline{p}^* = 1$ .

The amplitudes  $r_{s,p}$  and  $t_{1,2}$  of the reflected and transmitted plane waves are conveniently related to the amplitudes  $a_{s,p}$  of the incident plane wave via the matrix relations

$$\begin{bmatrix} r_s \\ r_p \end{bmatrix} = \begin{bmatrix} r_{ss} & r_{sp} \\ r_{ps} & r_{pp} \end{bmatrix} \begin{bmatrix} a_s \\ a_p \end{bmatrix}, \quad (17)$$

$$\begin{bmatrix} t_1 \\ t_2 \end{bmatrix} = \begin{bmatrix} t_{1s} & t_{1p} \\ t_{2s} & t_{2p} \end{bmatrix} \begin{bmatrix} a_s \\ a_p \end{bmatrix}. \quad (18)$$

In order to find the reflection and transmission coefficients ( $r_{ss}$  etc. and  $t_{1s}$  etc.), the boundary conditions

$$\left. \begin{aligned} [\underline{E}_i(\underline{r}) + \underline{E}_r(\underline{r}) - \underline{E}_t(\underline{r})] \cdot \hat{\underline{v}} &= 0 \\ [\underline{H}_i(\underline{r}) + \underline{H}_r(\underline{r}) - \underline{H}_t(\underline{r})] \cdot \hat{\underline{v}} &= 0 \end{aligned} \right\}, \quad z = 0; \quad v = x, y \quad (19)$$

are imposed. Thus, the four simultaneous linear algebraic equations

$$-a_p \cos \psi + r_p \cos \psi - t_2 \underline{p} \cdot \hat{\underline{x}} = 0, \quad (20)$$

$$a_s + r_s - t_1 = 0, \quad (21)$$

$$-\frac{a_s}{\eta_0} \cos \psi + \frac{r_s}{\eta_0} \cos \psi - t_1 \left[ \underline{\mu}^{-1} \cdot \left( \frac{1}{\omega} \underline{k}_1 \times \underline{I} - \underline{\zeta} \right) \cdot \underline{s} \right] \cdot \hat{\underline{x}} - t_2 \left[ \underline{\mu}^{-1} \cdot \left( \frac{1}{\omega} \underline{k}_2 \times \underline{I} - \underline{\zeta} \right) \cdot \underline{p} \right] \cdot \hat{\underline{x}} = 2\mathbf{Q},$$

$$-\frac{a_p}{\eta_0} - \frac{r_p}{\eta_0} - t_1 \left[ \underline{\mu}^{-1} \cdot \left( \frac{1}{\omega} \underline{k}_1 \times \underline{I} - \underline{\zeta} \right) \cdot \underline{s} \right] \cdot \hat{\underline{y}} - t_2 \left[ \underline{\mu}^{-1} \cdot \left( \frac{1}{\omega} \underline{k}_2 \times \underline{I} - \underline{\zeta} \right) \cdot \underline{p} \right] \cdot \hat{\underline{y}} = 0 \quad (23)$$

emerge, which may be solved to provide  $r_{ss}$  etc. and  $t_{1s}$  etc. by straightforward algebraic manipulations.

For the bianisotropic metamaterial considered here, it transpires that  $r_{sp} = r_{ps} = 0$  and  $t_{1p} = t_{2s} = 0$ . The absolute values of  $r_{ss}$ ,  $r_{pp}$ ,  $t_{1s}$  and  $t_{2p}$  are plotted against  $\kappa/k_0$  in Fig 4. The transmission coefficients have magnitudes  $> 1$  in the chosen representation of the transmitted fields, but we have verified that the principle of conservation of energy is satisfied by the results.

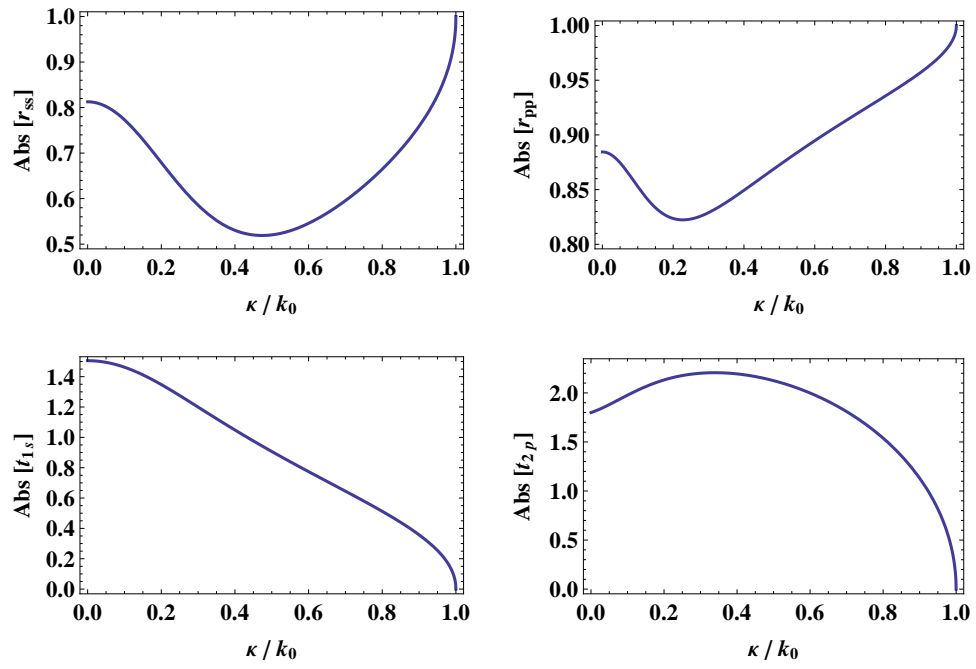


Figure 4: The absolute values of  $r_{ss}$ ,  $r_{pp}$ ,  $t_{1s}$  and  $t_{2p}$  plotted against  $\kappa/k_0$ .